

## SUPPLEMENTAL MATERIAL

### **Differential microRNA-21 and microRNA-221 upregulation in the biventricular failing heart reveals distinct stress responses of right versus left ventricular fibroblasts**

Jeffery C. Powers, Ph.D.; Abdelkarim Sabri, Ph.D.; Dalia Al-Bataineh, B.S.; Dhruv Chotalia, B.S.; Xinji Guo, Ph.D.; Florence Tsipenyuk, B.S.; Remus Berretta, B.S.; Pavithra Kavitha, B.S.; Heramba Gopi, B.S.; Steven R. Houser, Ph.D.; Mohsin Khan, Ph.D.; Emily J. Tsai, M.D.; Fabio A. Recchia, M.D., Ph.D.

#### **Supplemental Methods**

##### *Surgical instrumentation and pacing protocol*

Mongrel dogs (age: 9-13 months; weight: 21-27 kg) were anesthetized were maintained under anesthesia with 2% to 3% isoflurane and subjected to left thoracotomy along the fifth intercostal space. Then they were chronically instrumented with a solid-state pressure gauge inserted in the left ventricle, a fluid-filled catheter inserted in the descending thoracic aorta and two pacing leads attached to the left ventricular (LV) epicardial surface, as previously described (1-2). Wires and catheters were run subcutaneously to the intrascapular region. Antibiotics were given after surgery and the dogs were allowed to fully recover. After 10 days of post-surgical recovery, the dogs underwent cardiac pacing with an external pacemaker at the rate of 210 beats/min for 3 weeks and at 240 beats/min for an additional week to induce heart failure (HF), as previously described (1-2). All the hemodynamic and echo measurements were performed at baseline (before pacing was started) and every week in conscious, non-sedated dogs recumbent on the right side on the laboratory table. In total, cardiac pacing was maintained for 28-29 days. By this time point, LV end-diastolic pressure reached  $\geq 25$  mmHg, terminal measurements were performed, and the dog was euthanized for cardiac tissue harvesting and ex vivo analyses.

### *Hemodynamic and echocardiographic measurements*

HF dogs were studied at spontaneous heart rate, with the pacemaker turned off. During the terminal measurements, a 5F Swan-Ganz catheter was advanced through a leg vein to measure pressure in RV and pulmonary artery. LV pressure was measured using the implanted solid-state pressure gauge, while aortic pressure was measured by connecting the implanted fluid-filled catheter to a strain gauge. All signals were digitally stored via a custom made analog-digital interface at a sampling rate of 250Hz. Digitized data were analyzed off-line by commercially available software (Notocord hem evolution, Notocord). The data for each time point were obtained by averaging measures over  $\geq 4$  respiratory cycles.

Transthoracic echocardiography was performed in conscious dogs at baseline prior to onset of tachy-pacing and then weekly following onset of pacing protocol (1). To assess RV function, RV fractional area change was measured using B-mode imaging in the apical four-chamber view, given the irregular geometry of this chamber. To assess LV function, LV fractional area change was measured in the parasternal short axis view.

### *miRNA Microarray Analysis*

Total RNA, including miRNA, were extracted from LV and RV free wall tissue of control and HF dogs (n=3 per group) using Norgen Biotek Total RNA Purification Kit. Total RNA quantity and quality were analyzed by NanoDrop 2000c and submitted to LC sciences (Houston, TX) for subsequent sample quality control, processing, and hybridization with miRNA microarray ( $\mu$ Paraflo® Microfluidic Biochip Technology, Sanger canine miRBase v19.0). The miR microarray represented 289 distinct miR probes and 55 control probes. Standard Illumina base calling and data filtering were applied to remove low quality reads and background-subtracted

mappable reads were determined and normalized by an LC Sciences developed analysis program. miRNAs for which the mean signal of at least one group (i.e. LV-Ctrl, LV-HF, RV-Ctrl, RV-HF) was detectable ( $> 32$ ) were chosen for further analysis.

### *Histological analysis*

After deparaffinization and rehydration, 5  $\mu\text{m}$ -thick LV and RV tissue slices were treated in 0.2% phosphomolybdic acid for five minutes and stained with 0.1% Sirius Red in saturated picric acid for two hours. Collagen was stained red and quantified as a percentage of the visual field using ImageJ software (3).

### *Isolation of canine cardiac myocytes and fibroblasts*

LV and RV were enzymatically dissociated to isolate cells as previously described (4). Cardiomyocytes and fibroblasts were separated by adapting a protocol we previously used for rodent hearts (5). In brief, the left anterior descending coronary artery and the right coronary artery of excised hearts were cannulated to perfuse, respectively, a LV portion and the entire RV, and mounted on a constant-flow Langendorff apparatus for retrograde perfusion with collagenase-containing Krebs-Henseleit buffer (180 U/mL) supplemented with 50  $\mu\text{M}$   $\text{CaCl}_2$ . When the tissue softened, the LV and RV perfused areas were excised and gently minced and filtered. The cell suspension was then centrifuged and the supernatant, containing fibroblasts, was aspirated and centrifuged a second time at 1500 rpm for 5 minutes. The pellet from each centrifugation (the first being myocytes, the second being fibroblasts) was resuspended in DMEM (Sigma) and plated in collagen I-coated elastic well plates (Flex-Cell).

### *Flow cytometry confirmation of isolated cardiac fibroblast purity*

Two-color flow cytometry was performed to verify the purity of isolated fibroblasts. Cells were labeled to detect the following cell type markers: fibroblast-specific protein 1 (FSP1) and platelet-derived growth factor- $\alpha$  (PDGF- $\alpha$ ) for fibroblasts;  $\alpha$ -smooth muscle actin ( $\alpha$ -SMA) for myofibroblasts and smooth muscle cells; CD31 for endothelial cells; and CD45 for leukocytes. Unconjugated primary antibodies were used for the fibroblast, myofibroblast, and smooth muscle cell markers, followed by PE-conjugated secondary antibodies. FITC-conjugated primary antibodies were used for the endothelial and leukocyte markers. Flow cytometry analysis was performed using an LSR II Flow Cytometer (BD Biosciences) and FlowJo software (6).

### *Cyclic stretch and neurohormonal stimulation of isolated cardiomyocytes and fibroblasts*

Cardiomyocytes and fibroblasts were separately incubated at 37 °C and 5% CO<sub>2</sub> for 48 hours and then subjected to cyclic stretch and/or aldosterone treatment to simulate two stressors that importantly contribute to cell injury and fibrosis in the failing heart (7-11). For the cyclic stretch protocol, the Flex-Cell FX-5000 Tension System, Trivac D8B Vacuum System, and Flex-Cell Pressure Reservoir were used. Plates were loaded into Flex-Cell baseplate (housed in a 37°C incubator at 95% O<sub>2</sub>/5% CO<sub>2</sub>) and a Plexiglas cover was added to seal it. The system was then programmed to stretch cells at 15% at 1 Hz for 24 hours, i.e. the total time of incubation at 37 °C, to simulate pathological strain in vivo (7). Unstretched cell plates (control) were placed in the same incubator. For aldosterone treatment, we used a concentration of 250 pg/ml (694 pM) in the culture medium and the cells were incubated at 37 °C for 24 hours. We chose a concentration of aldosterone that mimics mild pathophysiological blood levels found in HF patients (8) and similar

to the one used in other in vitro studies (9-10). The effects of 15% stretch and 250 pg/ml aldosterone were also tested in combination in a separate set of cell culture experiments.

#### *RT-qPCR and Western analyses*

Total mRNA, including miRNA, and total protein were extracted from cell lysates using the MiRVana RNA Isolation Kit (Ambion) and Cell Lysis Buffer (Cell Signaling Technology), respectively. Reverse transcription was performed using the miScript II RT Kit (Qiagen). RT-qPCR was performed using miScript Primer Assays for microRNA, RT2 qPCR Primer Assays for messenger RNA, and QuantiTect SYBR Green PCR Kits (Qiagen). Western blot analysis was performed as previously described (2). Proteins of interest were probed with primary antibodies for phosphatase and tensin homologue (PTEN), Spry1 and  $\beta$ -actin (Pro-Sci). Secondary antibodies were anti-mouse or anti-rabbit IRDye 680RD (LI-COR). Membranes were scanned with a LI-COR Odyssey Imaging system and images were analyzed using Image Studio software.

**Supplemental Table 1. Summary of miRNA Microarray Data**

Reporter Name	LV-Ctrl		LV-HF		RV-Ctrl		RV-HF		Fold Change (RV-HF/RV-Ctrl)	Log2 (RV-HF/RV-Ctrl)	RV-HF vs. RV-Ctrl p-value	Fold Change (LV-HF/LV-Ctrl)	Log2 (LV-HF/LV-Ctrl)	LV-HF vs. LV-Ctrl p-value	Fold Change (RV-HF/LV-HF)	Log2 (RV-HF/LV-HF)	RV-HF vs. LV-HF p-value
	Mean	SD	Mean	SD	Mean	SD	Mean	SD									
cfa-let-7a	6,105	4,530	5,417	1,209	5,430	1,504	5,006	1,246	0.92	-0.12	7.26E-01	0.89	-0.17	8.12E-01	0.92	-0.12	7.02E-01
cfa-let-7b	3,219	2,074	2,960	1,163	2,655	818	2,703	514	1.02	0.03	9.36E-01	0.92	-0.12	8.59E-01	0.95	-0.07	7.45E-01
cfa-let-7c	3,295	2,357	3,241	807	3,411	1,249	2,960	445	0.87	-0.20	5.87E-01	0.98	-0.02	9.72E-01	0.92	-0.11	6.25E-01
cfa-let-7e	864	470	914	167	1,324	928	660	116	0.50	-1.00	2.87E-01	1.06	0.08	8.70E-01	0.72	-0.47	9.60E-02
cfa-let-7f	6,004	4,397	5,692	925	5,952	1,782	5,219	1,386	0.88	-0.19	6.04E-01	0.95	-0.08	9.10E-01	0.90	-0.15	6.49E-01
cfa-let-7g	5,179	963	5,468	260	5,662	918	5,272	773	0.93	-0.10	6.04E-01	1.06	0.08	6.43E-01	0.96	-0.06	7.00E-01
cfa-let-7j	3	3	3	1	6	2	2	1									
<b>cfa-miR-1</b>	10,733	3,940	17,212	6,458	20,843	4,024	14,693	458	0.70	-0.50	5.82E-02	1.60	0.68	2.12E-01	0.90	-0.16	5.37E-01
cfa-miR-7	18	11	43	12	26	2	58	26	2.21	1.14	1.01E-01	2.35	1.23	6.17E-02	1.29	0.37	4.13E-01
cfa-miR-9	15	11	12	2	19	7	9	3									
<b>cfa-miR-10a</b>	304	254	97	79	175	85	35	12	0.20	-2.30	4.86E-02	0.32	-1.65	2.48E-01	0.48	-1.05	2.54E-01
cfa-miR-10b	325	119	432	160	646	278	382	135	0.59	-0.76	2.13E-01	1.33	0.41	4.10E-01	0.90	-0.15	7.01E-01
cfa-miR-15a	335	153	395	150	537	59	459	120	0.85	-0.23	3.71E-01	1.18	0.24	6.48E-01	1.19	0.24	6.01E-01
cfa-miR-15b	248	76	368	168	614	420	408	88	0.66	-0.59	4.52E-01	1.48	0.57	3.23E-01	1.16	0.22	7.31E-01
<b>cfa-miR-16</b>	3,045	486	3,139	705	2,902	149	3,358	298	1.16	0.21	7.63E-02	1.03	0.04	8.58E-01	1.09	0.12	6.47E-01
cfa-miR-17	7	3	2	1	3	2	5	1									
cfa-miR-18a	17	5	13	2	12	4	19	4									
cfa-miR-18b	10	8	6	3	6	4	10	1									
cfa-miR-19a	24	20	40	41	30	22	34	19	1.15	0.20	8.10E-01	1.66	0.73	5.92E-01	1.09	0.13	8.31E-01
cfa-miR-19b	281	308	305	235	280	198	286	92	1.02	0.03	9.68E-01	1.09	0.12	9.19E-01	1.12	0.16	8.99E-01
<b>cfa-miR-20a</b>	719	119	631	24	563	134	776	39	1.38	0.46	5.75E-02	0.88	-0.19	2.74E-01	1.23	0.30	5.55E-03
<b>cfa-miR-20b</b>	394	32	380	14	303	63	462	75	1.52	0.61	4.87E-02	0.97	-0.05	5.27E-01	1.20	0.27	1.38E-01
<b>cfa-miR-21</b>	1,913	943	3,825	764	2,608	1,829	10,215	5,060	3.92	1.97	7.05E-02	2.00	1.00	5.25E-02	2.48	1.31	9.66E-02
cfa-miR-22	6,018	776	6,193	965	4,758	1,546	5,986	436	1.26	0.33	2.56E-01	1.03	0.04	8.19E-01	0.97	-0.04	7.53E-01
cfa-miR-23a	4,379	1,640	7,664	2,094	7,676	1,238	6,935	222	0.90	-0.15	3.65E-01	1.75	0.81	9.91E-02	0.93	-0.11	5.81E-01
cfa-miR-23b	3,665	1,621	6,001	2,311	6,561	1,458	5,435	143	0.83	-0.27	2.54E-01	1.64	0.71	2.25E-01	0.95	-0.07	6.93E-01
cfa-miR-24	11,435	375	13,139	2,614	9,056	2,702	12,451	797	1.37	0.46	1.05E-01	1.15	0.20	3.26E-01	0.96	-0.06	6.85E-01
cfa-miR-25	995	171	722	81	800	261	772	152	0.97	-0.05	8.83E-01	0.73	-0.46	6.68E-02	1.06	0.08	6.42E-01
cfa-miR-26a	13,240	1,437	13,269	2,212	12,940	782	13,388	1,435	1.03	0.05	6.61E-01	1.00	0.00	9.85E-01	1.01	0.02	9.42E-01
cfa-miR-26b	3,030	756	3,564	433	4,691	1,223	3,455	178	0.74	-0.44	1.58E-01	1.18	0.23	3.49E-01	0.97	-0.04	7.07E-01
cfa-miR-27a	4,225	852	5,205	1,172	4,650	640	4,509	503	0.97	-0.04	7.78E-01	1.23	0.30	3.07E-01	0.88	-0.19	3.98E-01
cfa-miR-27b	5,156	305	5,852	913	4,548	288	4,588	508	1.01	0.01	9.12E-01	1.13	0.18	2.79E-01	0.79	-0.34	1.04E-01
cfa-miR-28	162	25	160	47	124	33	149	25	1.20	0.27	3.47E-01	0.99	-0.02	9.67E-01	0.95	-0.07	7.36E-01
cfa-miR-29a	3,097	296	3,256	441	3,060	670	2,871	466	0.94	-0.09	7.09E-01	1.05	0.07	6.31E-01	0.88	-0.19	3.56E-01
cfa-miR-29b	313	214	508	461	590	313	348	131	0.59	-0.76	2.85E-01	1.62	0.70	5.45E-01	0.86	-0.22	5.96E-01
cfa-miR-29c	2,376	1,109	2,351	828	3,116	871	2,047	562	0.66	-0.61	1.49E-01	0.99	-0.02	9.76E-01	0.89	-0.18	6.26E-01
cfa-miR-30a	5,746	1,187	5,604	504	5,945	1,227	4,972	335	0.84	-0.26	2.56E-01	0.98	-0.04	8.58E-01	0.89	-0.17	1.45E-01
<b>cfa-miR-30b</b>	6,879	370	5,243	458	6,074	451	5,161	483	0.85	-0.23	7.50E-02	0.76	-0.39	8.60E-03	0.98	-0.02	8.42E-01
cfa-miR-30c	7,122	466	6,874	398	7,641	268	6,866	718	0.90	-0.15	1.55E-01	0.97	-0.05	5.22E-01	1.00	-0.01	9.87E-01
cfa-miR-30d	7,518	587	6,902	171	7,169	374	6,381	691	0.89	-0.17	1.57E-01	0.92	-0.12	1.56E-01	0.92	-0.12	2.73E-01
<b>cfa-miR-30e</b>	424	156	437	147	696	143	395	52	0.57	-0.82	2.63E-02	1.03	0.05	9.19E-01	0.94	-0.10	6.64E-01
cfa-miR-31	251	61	171	13	185	46	143	40	0.78	-0.37	3.00E-01	0.68	-0.55	9.18E-02	0.82	-0.29	3.08E-01
cfa-miR-32	5	7	3	1	2	1	5	2									
cfa-miR-33a	2	1	4	2	2	1	1	0									
cfa-miR-33b	1	1	3	1	2	2	2	1									
cfa-miR-34a	325	105	182	63	190	67	183	20	0.96	-0.05	8.70E-01	0.56	-0.84	1.15E-01	1.04	0.06	9.87E-01
cfa-miR-34b	2	1	4	2	3	1	4	4									
cfa-miR-34c	2	2	7	3	3	2	3	2									
cfa-miR-92a	1,763	302	1,508	297	1,835	674	1,880	288	1.02	0.03	9.21E-01	0.85	-0.23	3.55E-01	1.25	0.33	1.94E-01
cfa-miR-92b	567	70	520	55	732	318	657	62	0.90	-0.16	7.06E-01	0.92	-0.12	4.19E-01	1.26	0.34	4.57E-02
<b>cfa-miR-93</b>	509	48	381	42	315	55	445	19	1.41	0.50	1.76E-02	0.75	-0.42	2.52E-02	1.17	0.23	7.37E-02
<b>cfa-miR-95</b>	10	6	27	14	38	8	12	6	0.32	-1.65	1.31E-02	2.77	1.47	1.08E-01	0.44	-1.19	1.52E-01
cfa-miR-96	2	1	3	0	2	3	1	1									
cfa-miR-98	229	174	247	21	272	138	194	39	0.71	-0.49	4.02E-01	1.08	0.11	8.72E-01	0.78	-0.37	1.09E-01
cfa-miR-99a	3,320	508	3,070	603	3,978	887	3,571	430	0.90	-0.16	5.15E-01	0.92	-0.11	6.12E-01	1.17	0.23	3.06E-01
cfa-miR-99b	807	299	725	208	814	258	762	74	0.94	-0.10	7.54E-01	0.90	-0.15	7.17E-01	1.07	0.10	7.87E-01







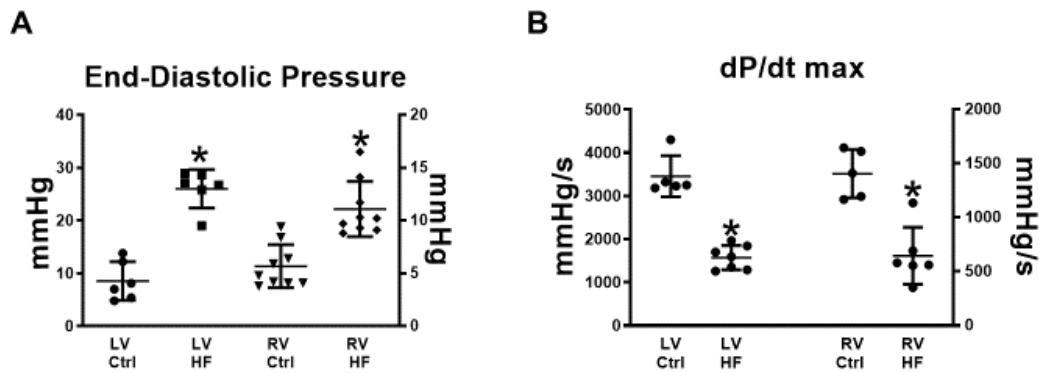




**Supplemental Table 1 (continued)**

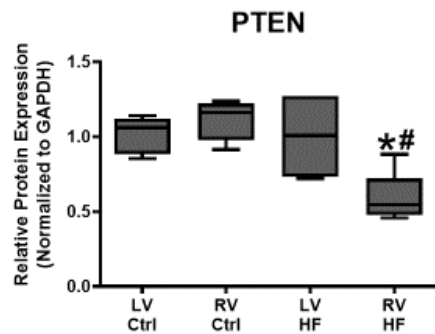
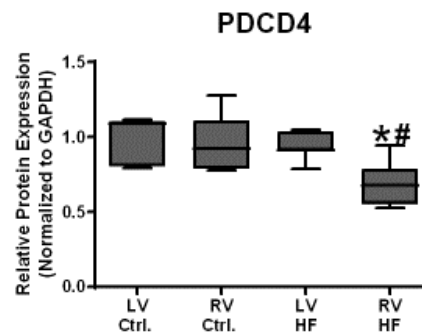
Reporter Name	LV-Ctrl		LV-HF		RV-Ctrl		RV-HF		Fold Change (RV-HF/RV-Ctrl)	Log2 (RV-HF/RV-Ctrl)	RV-HF vs. RV-Ctrl p-value	Fold Change (LV-HF/LV-Ctrl)	Log2 (LV-HF/LV-Ctrl)	LV-HF vs. LV-Ctrl p-value	Fold Change (RV-HF/LV-HF)	Log2 (RV-HF/LV-HF)	RV-HF vs. LV-HF p-value	
	Mean	SD	Mean	SD	Mean	SD	Mean	SD										
cfa-miR-885	3	2	7	5	7	4	6	1										
cfa-miR-1271	160	23	146	29	135	32	124	23	0.92	-0.12	6.77E-01	0.91	-0.13	5.52E-01	0.85	-0.23	3.75E-01	
cfa-miR-1306	104	25	93	19	88	15	89	8	1.01	0.01	9.51E-01	0.89	-0.16	5.65E-01	0.97	-0.05	7.77E-01	
cfa-miR-1307	129	33	102	8	89	33	109	32	1.22	0.29	4.99E-01	0.79	-0.34	2.42E-01	1.04	0.06	7.26E-01	
cfa-miR-1835	479	126	429	180	488	326	208	149	0.43	-1.23	2.47E-01	0.89	-0.16	7.10E-01	0.42	-1.25	1.77E-01	
cfa-miR-1836	5	7	3	2	3	2	1	1										
cfa-miR-1837	13	7	3	2	4	2	2	3										
cfa-miR-1838	24	4	34	15	15	6	21	15	1.35	0.43	6.31E-01	1.40	0.48	3.54E-01	0.54	-0.88	3.52E-01	
cfa-miR-1839	9	6	13	5	7	5	7	3										
cfa-miR-1840	12	2	5	3	7	3	6	8										
cfa-miR-1841	9	2	3	2	10	6	4	4										
cfa-miR-1842	13	6	6	3	7	4	8	6										
cfa-miR-1843	12	3	8	4	8	2	9	5										
cfa-miR-1844	186	26	164	123	219	151	103	49	0.47	-1.08	2.78E-01	0.88	-0.18	7.76E-01	0.74	-0.43	4.71E-01	

## Supplemental Figures and Figure Legends

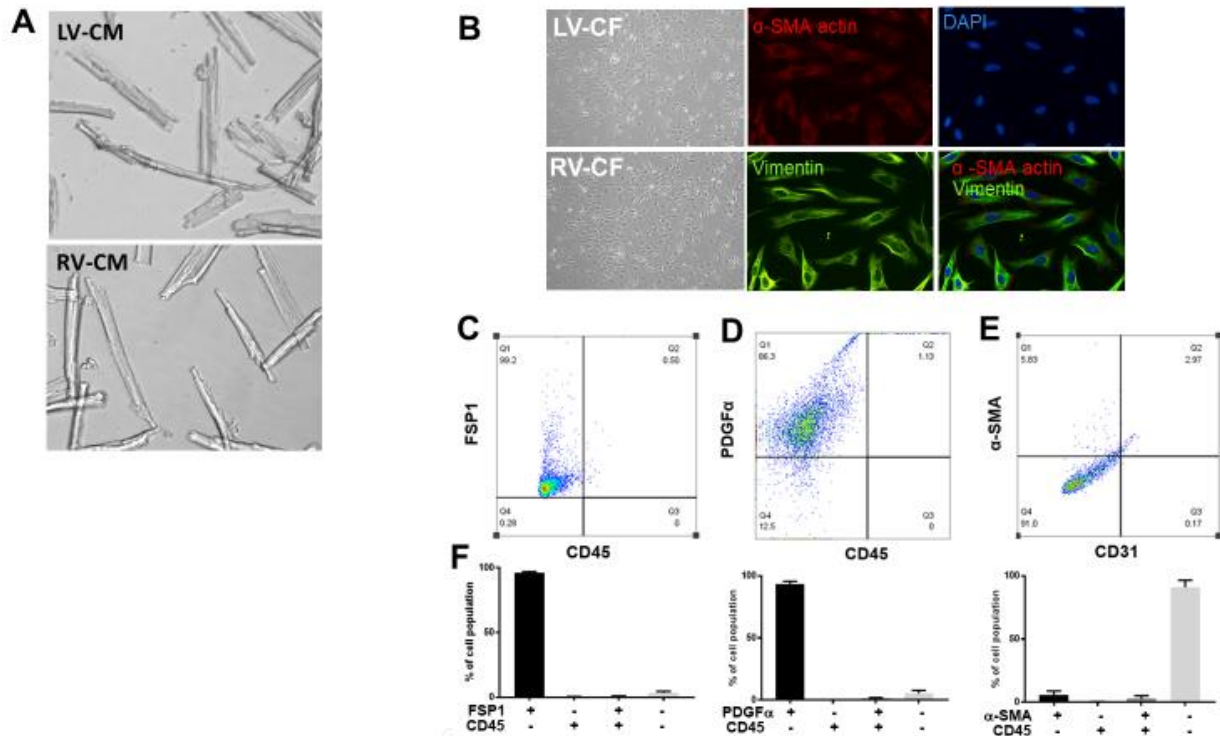


### Supplemental Figure 1. Invasive hemodynamic measurements obtained in tachy-pacing

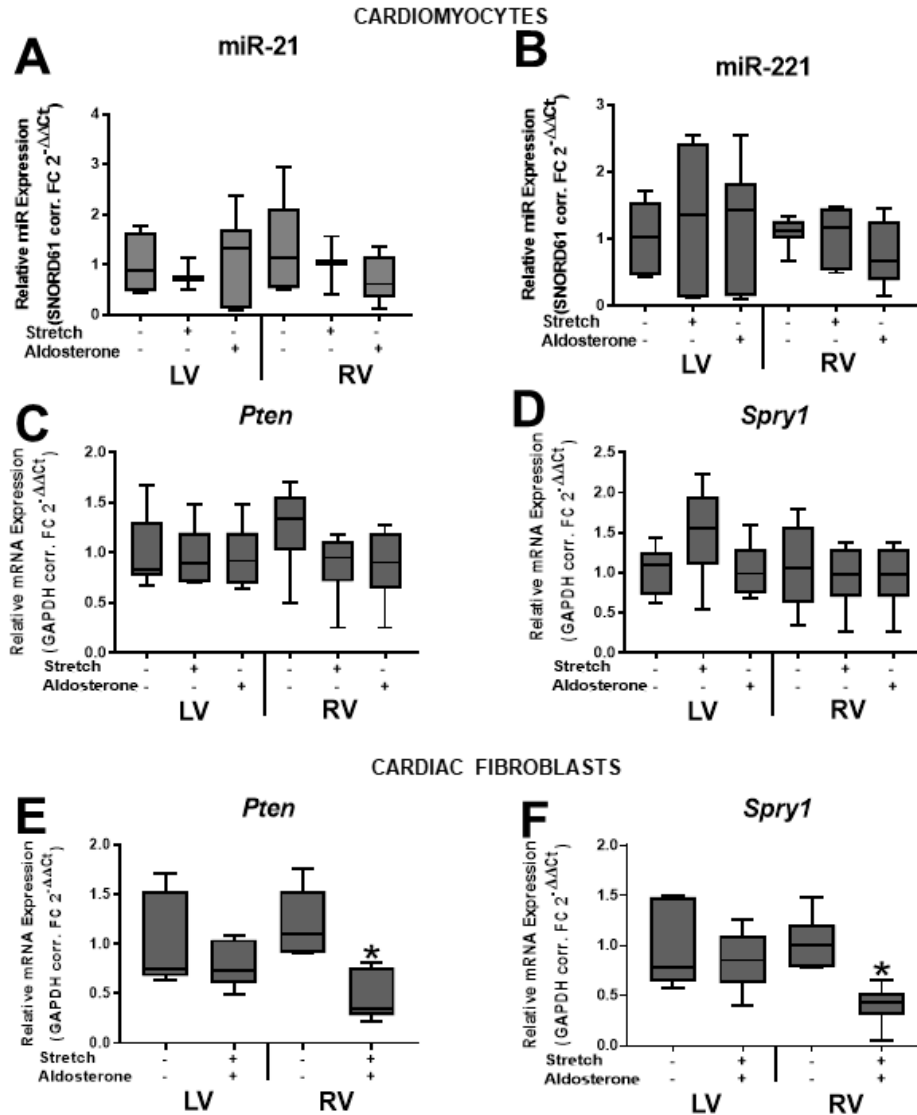
(**HF**) and control (**Ctrl**) dogs. (**A**) In HF animals, both LV and RV end-diastolic pressures are elevated while (**B**) LV and RV contractility (dP/dtmax) are depressed. \* $P < 0.001$  vs respective Ctrl.

**A****B**

**Supplemental Figure 2. miR-21/-221 targets PTEN and PDCD4 are downregulated in the failing RV.** Protein expression of miR-21 and miR-221 targets (A) phosphatase and tensin homologue (PTEN) and (B) programmed cell death-4 (PDCD4) were decreased in the RV of tachy-pacing HF animals, n= 6 per group. \* $P < 0.05$  vs respective Ctrl; # $P < 0.05$  vs LV HF.



**Supplemental Figure 3. Isolated adult canine cardiomyocytes and fibroblasts used for in vitro studies.** (A) Representative cardiomyocytes (CM) isolated from LV and RV that were subjected to cyclic overstretch and/or exposed to aldosterone. (B) Phase contrast micrographs of fibroblasts (CF) isolated from LV and RV and cultured for 48 h. LV and RV fibroblasts were stained for myofibroblast/smooth muscle marker  $\alpha$ -smooth muscle actin ( $\alpha$ -SMA), fibroblast marker vimentin, and nuclear stain DAPI to verify their cell type. Purity of isolated fibroblasts was confirmed by FACS analysis based upon the presence of fibroblast markers (C) fibroblast-specific protein 1 (FSP1) and (D) platelet-derived growth factor- $\alpha$  (PDGF- $\alpha$ ) and the absence of (E)  $\alpha$ -SMA, endothelial marker CD31, and leukocyte marker CD45. (F) Summary FACS analysis confirms virtual purity of isolated fibroblasts.



**Supplemental Figure 4.** Neither cyclic stretch nor aldosterone affected expression of miR-21/-221 or their targets *Pten* and *Spry1* in isolated cardiac myocytes, but they did induce changes in RV fibroblasts that were consistent with their miR-21/-221 expression. LV and RV cardiomyocytes (CM) and fibroblasts (FB) were subjected to cyclic overstretch and/or exposed to aldosterone for 24h. Expression of (A) miR-21, (B) miR-221, and their target mRNAs (C) *Pten* and (D) *Spry1* in isolated CMs. mRNA expression of miR-21/-221 targets (E) *Pten* and (F) *Spry1* in isolated FBs. n=12 for each experimental condition. \* $P < 0.05$  vs unstimulated RV.

## Supplemental References

1. Woitek F, Zentilin L, Hoffman NE, Powers JC, Ottiger I, Parikh S, Kulczycki AM, Hurst M, Ring N, Wang T, Shaikh F, Gross P, Singh H, Kolpakov MA, Linke A, Houser SR, Rizzo V, Sabri A, Madesh M, Giacca M, Recchia FA. Intracoronary Cytoprotective Gene Therapy: A Study of VEGF-B167 in a Pre-Clinical Animal Model of Dilated Cardiomyopathy. *J Am Coll Cardiol*. 2015;66:139-53.
2. Seki M, Powers JC, Maruyama S, Zuriaga MA, Wu CL, Kurishima C, Kim L, Johnson J, Poidomani A, Wang T, Muñoz E, Rajan S, Park JY, Walsh K, Recchia FA. Acute and Chronic Increases of Circulating FSTL1 Normalize Energy Substrate Metabolism in Pacing-Induced Heart Failure. *Circ Heart Fail*. 2018;11:e004486.
3. Kolpakov MA, Seqqat R, Rafiq K, Xi H, Margulies KB, Libonati JR, Powel P, Houser SR, Dell'italia LJ, Sabri A. Pleiotropic effects of neutrophils on myocyte apoptosis and left ventricular remodeling during early volume overload. *J Mol Cell Cardiol*. 2009;47:634-45.
4. Dubell WH, Houser SR. Voltage and beat dependence of Ca<sub>2+</sub> transient in feline ventricular myocytes. *Am J Physiol*, 1989;257:H746-59
5. Hooshdaran B, Kolpakov MA, Guo X, Miller SA, Wang T, Tilley DG, Rafiq K, Sabri A. Dual inhibition of cathepsin G and chymase reduces myocyte death and improves cardiac remodeling after myocardial ischemia reperfusion injury. *Basic Res Cardiol*. 2017;112:62.
6. Tallquist MD, Molkentin JD. Redefining the identity of cardiac fibroblasts. *Nat Rev Cardiol*. 2017;14:484-491.
7. Lindner D, Zietsch C, Tank J, Sossalla S, Fluschnik N, Hinrichs S, Maier L, Poller W, Blankenberg S, Schultheiss HP, Tschöpe C, Westermann D. Cardiac fibroblasts support cardiac inflammation in heart failure. *Basic Res Cardiol*. 2014;109:428.
8. Knight RK, Miall PA, Hawkins LA, Dacombe J, Edwards CR, Hamer J. Relation of plasma aldosterone concentration to diuretic treatment in patients with severe heart disease. *Br Heart J*. 1979;42:316-25
9. Brilla CG, Zhou G, Matsubara L, Weber KT. Collagen metabolism in cultured adult rat cardiac fibroblasts: response to angiotensin II and aldosterone. *J Mol Cell Cardiol*. 1994;26:809-20.
10. Neumann S, Huse K, Semrau R, Diegeler A, Gebhardt R, Buniatian GH, Scholz GH. Aldosterone and D-glucose stimulate the proliferation of human cardiac myofibroblasts in vitro. *Hypertension*. 2002;39:756-60.
11. Zannad F, Alla F, Dousset B, Perez A, Pitt B. Limitation of excessive extracellular matrix turnover may contribute to survival benefit of spironolactone therapy in patients with congestive heart failure: insights from the randomized aldactone evaluation study (RALES). Rales Investigators. *Circulation*. 2000;102:2700-6.